Pulsed NMR studies of self-diffusion and defect structure in liquid and solid krypton*†

Donald F. Cowgill‡ and Richard E. Norberg
Department of Physics, Washington University, St. Louis, Missouri 63130
(Received 11 November 1975)

Nuclear spin-spin relaxation and atomic self-diffusion have been studied for ^{83}Kr in liquid and solid natural krypton. Transient NMR signals observed in the solid phase are separated into components governed by the effective quadrupolar and dipolar interactions. Interpretation of the quadrupolar component is aided by the analysis of observed quadrupole echoes. Fedders's calculations of quadrupolar effects for spin 9/2 are found to agree with ^{83}Kr central transition relaxation rates observed in solid krypton. Analyses of motional narrowing indicate the coefficient of atomic self-diffusion in solid krypton to be $D = 3.1^{+6.8}_{-2.1}\exp[-(5010 \pm 220)/RT]$ cm^2/sec. In liquid krypton, direct external-gradient self-diffusion measurements yield $D\rho = (1.83 \pm 0.25) \times 10^{-3}\exp[-(180 \pm 40)/RT]$ g/cm sec.

I. INTRODUCTION

Magnetic nuclides with nonzero nuclear electric quadrupole moments present favorable cases for gaining information about structural defects and internal motions in solids and liquids from the transient signals generated by pulsed nuclear magnetic resonance. Here spin-spin relaxation can proceed via the interaction of the quadrupole moment with electric field gradients generated by distortions of the atomic structure as well as via the magnetic dipole-dipole interaction. Gradient strengths and distributions, in turn, can provide information about the types and densities of the structural defects producing these distributions.[1-4]

The condensed phases of the rare gases form simple systems for line-shape studies. Environmentally produced distortions of the atomic structure have been found to be well characterized by weak van der Waals and electronic exchange forces.[5,6] Quadrupole structure has been previously observed and studied for the ^{131}Xe nuclide in solid xenon.[7] Motional narrowing of the dipolar-broadened central $-\frac{1}{2} \rightarrow \frac{1}{2}$ transition has been followed in xenon[7,8] and neon.[9,10] For the remaining abundant magnetic rare-gas nuclide ^{83}Kr no line-shape studies have been reported. Self-diffusion in krypton has been measured at various densities using radioactive-tracer techniques.[11-13] The thermal activation energy so obtained in solid krypton appears to be 10% low when compared with the other rare gases by corresponding-states analysis.[9]

The present paper describes the results of pulsed NMR measurements of the nuclear spin-spin relaxation of ^{83}Kr in solid and liquid natural krypton between 40 K and the critical point (209.4 K at 54.3 atm) under saturated vapor pressure.[14] It is shown that under certain conditions the relaxation may be resolved into a two-component decay characterized by two time constants describing the effective dipolar and quadrupolar interactions. The quadrupole splitting in the rigid solid also is determined by analysis of the quadrupole echo shape. From these data, information is obtained concerning the nature and motion of lattice defects in the solid.

In the preceding paper,[15] Fedders has calculated some striking effects of large first-order static quadrupole splittings on the rate $1/T_2$ observed for a central $-\frac{1}{2} \rightarrow \frac{1}{2}$ transition. We have applied Fedder's theory to analyses of our ^{83}Kr T_2 data in solid krypton and find that the theory correctly predicts the T_1/T_2 ratio observed in the hot solid. The analyses also yield a determination of the coefficient of atomic self-diffusion in solid krypton.

The results of NMR measurements of self-diffusion in the liquid also are presented and compared with tracer studies. Data on the ^{83}Kr spin-lattice relaxation and chemical shift obtained simultaneously with the present measurements have been reported previously.[5]

II. EXPERIMENTAL DETAILS

^{83}Kr (spin $\frac{9}{2}$) is 11.55% abundant in natural krypton and has a relatively small gyromagnetic ratio. In order to obtain an adequate signal-to-noise ratio, the measurements described here were performed with an 8.475-MHz pulsed NMR spectrometer constructed around a 51.6-kG superconducting solenoid. Most of this apparatus has been described in Ref. 5. The power transmitter was capable of providing 80-G rotating-frame pulses of two different and adjustable phases relative to the reference supplying the phase-sensitive detector. The pulses used were short enough that their spectra well covered the NMR line structure. The pulse logic used to control the gated pulse amplifier also controlled a gated magnetic field

gradient which was applied to the sample for the liquid self-diffusion measurements. The gradient was generated by two opposing 1-in.-diam coils wound on the probe can which enclosed the sample chamber. Gating the gradient was necessary to minimize resistive heating of the can. The 1.75-in.-diam superconducting shield (provided by the solenoid) which surrounded the can was found to improve the gradient linearity over the sample relative to the isolated coil configuration. From spin-echo shape analysis it was estimated that for gradients 100 times the natural magnetic linewidth the linearity was within 5% for the bulk of the spins, compared with 20% computed without the shield. Gradient magnitudes were obtained for the diffusion data by fitting the echo shapes in the liquid with a $J_1(\gamma Grt)/\gamma Grt$ function,[16] where J_1 is the first-order Bessel function and r is the sample radius. Gradients determined by this method are about 5% uncertain, because of the function's sensitivity to the gradient distribution. The gradients typically used were of the order of 45 G/cm, whereas the solenoid's inhomogeneity was $\frac{1}{3}$ G/cm over the $\frac{1}{2}$-cm^3 sample.

In the liquid phase, T_2 data were obtained with ($90°$-τ-$180°_{90°}$-2τ-$180°_{90°}$-$\cdots$) pulse sequences. The echo envelopes were least-squares fitted to exponentials and corrected for the diffusion contribution (less than 5%) resulting from the use of finite τ's. Three-pulse sequences ($90°$-τ_1-$180°_{90°}$-τ_2-$180°_{90°}$) were used for the self-diffusion measurements. Here, ratios of the echo pairs generated for various echo separations, $2\tau_2$-$2\tau_1$, were corrected for the T_2 decay and least-squares fitted to the function

$$\frac{S(2\tau_2)}{S(2\tau_1)} = \exp\left(-\frac{2\tau_2 - 2\tau_1}{T_2}\right) \exp - \left[\tfrac{1}{12}\gamma^2 G^2 D(2\tau_2 - 2\tau_1)^3\right],$$

where G is the magnetic field gradient and D is the diffusion coefficient.

T_2 relaxation times in the solid phase were deduced from the envelopes of $90°$-τ-$180°_{90°}$ echoes. Resolution of a rapid "quadrupolar" decay component was improved by narrowing the short-2τ echoes with pulsed magnetic field gradients. This was shown experimentally to produce no measurable effect on the envelope. Quadrupole 2τ echoes were generated with $90°$-τ-$\beta_{90°}$ pulse sequences. β-pulse angles were determined by comparing the pulse areas photographed from an oscilloscope. All pulse sequences were spaced by at least $5T_1$ and all measurements were made at resonance.

The cryogenic techniques used for these studies have been described elsewhere.[5] The accuracy of the sample temperature calibration was estimated at ±0.2 K; however, temperature differences between successive measurements were determined within ±10 mK. Temperature uniformity over the sample was estimated to be better than 1 mK. All data given in this paper are for pure krypton samples (<1.7-ppm O_2).

III. RESULTS IN SOLID

A. Analysis of echo envelope

The spin-spin relaxation of ^{83}Kr in polycrystalline solid krypton was measured between 40 K and the triple point, 115.78 K. To well within the accuracy of the data, the echo envelopes were found to be characterized by an initial rapid exponential decay superimposed on a slower exponential decay. Since ^{83}Kr (spin $\frac{9}{2}$) has a substantial nuclear quadrupole moment, these decays were interpreted, respectively, as arising from quadrupole splitting of the resonance structure and from the central transition. The corresponding decay time constants were labeled T_{2q} and T_{2c}.

Justification of this simple interpretation can be provided by considering the spectrum of an $I = \frac{9}{2}$ spin system in which the quadrupole interaction is strong compared to the dipole interaction. To first order the response can be described by a central unshifted line surrounded by four sets of satellites, each line dipolar broadened. For a Lorentzian dipolar broadening of half-width δ,[17]

$$g(\omega) = \frac{\delta}{\pi} \sum_{n=-4}^{+4} \frac{A_n}{\delta^2 + (\omega - \omega_0 + n\Delta)^2}. \tag{1}$$

Here $\Delta = \frac{1}{24} eQV_{zz}$ is the spacing between the lines and $A_n = A_{-n}$ are constants giving their relative intensities. Fourier transforming and integrating over a normalized distribution of field gradients $f(a)$, where $2a = \Delta$, gives the free induction decay or envelope of Hahn echoes,[18]

$$S(t) \propto e^{-\delta t}\left(A_0 + 2\sum_{n=1}^{4} A_n \int_{-\infty}^{+\infty} f(a)\cos(2nat)\,da\right). \tag{2}$$

The line intensities can be found by following the time evolution of the spin-density matrix under the first-order quadrupole interaction Hamiltonian, $\hbar H_q = \sum_i a_i I_{zi}^2$. A straightforward calculation gives the normalized nuclear signal following a $90°$ pulse,

$$S(t)_{\mathrm{FID}} = S_0 e^{-\delta t}(0.152 + 0.291F_1 + 0.255F_2 + 0.194F_3 + 0.109F_4), \tag{3}$$

where the F_n are the Fourier transforms of the electric-field-gradient distribution function $f(a,t)$,

$$F_n(t) = \int_{-\infty}^{\infty} f(a,t)\cos(2nat)\,da\,.$$

Using the same procedure, Mehring and Kanert[19] have examined the amplitude of the 2τ echo generated by a $90°$-τ-$\beta_{90°}$ pulse sequence in the presence of static magnetic dipolar and electric quadrupolar interactions. They find that for an $I=\frac{9}{2}$ solid, a maximum echo amplitude is expected for $\beta=24°$. Here there is a strong contribution from the satellite transitions; whereas for $\beta=180°$, at long τ only the central transition contributes to the echo. Thus considerable information on the distribution of field gradients is contained in the $90°$-τ-$24°_{90°}$ 2τ echo. Including the slow dipolar decay yields the compound echo shape

$$S(2\tau\pm t)_{CE} = S_0 e^{-\delta(2\tau\pm t)}(0.155+0.293F_1+0.264F_2 + 0.199F_3+0.089F_4)\,. \quad (4)$$

It was found experimentally that in the krypton rigid lattice a maximum ^{83}Kr echo was obtained for $\beta=24°$. An analysis of the shape of this echo is shown in Fig. 1. The plotted points $S(2\tau\pm t)$ have been deduced from the observed echo shape $E(2\tau\pm t)$ at 70.1 K by correcting for the magnet decay using

$$E(2\tau\pm t) = S(2\tau\pm t)M(2\tau\pm t)\,. \quad (5)$$

Here $M(2\tau\pm t)$ is the shape produced by the magnet inhomogeneity as determined from 2τ-echo shapes in the liquid, where the quadrupole broadening is averaged to zero by rapid motion. Also shown is the theoretical compound echo shape, Eq. (4), for

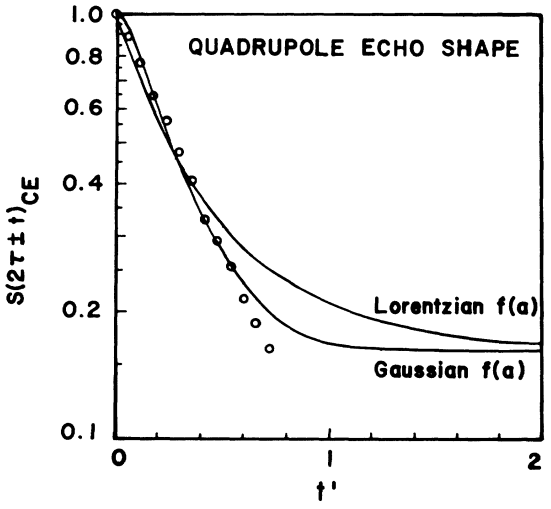

FIG. 1. Shape of the $90°$-τ-$24°_{90°}$ quadrupole echo. The solid lines are the theoretical shapes for Gaussian ($t'=\xi t/\sqrt{2}$) and Lorentzian ($t'=\lambda t$) electric-field-gradient distributions. The experimentally observed shape is plotted as data points.

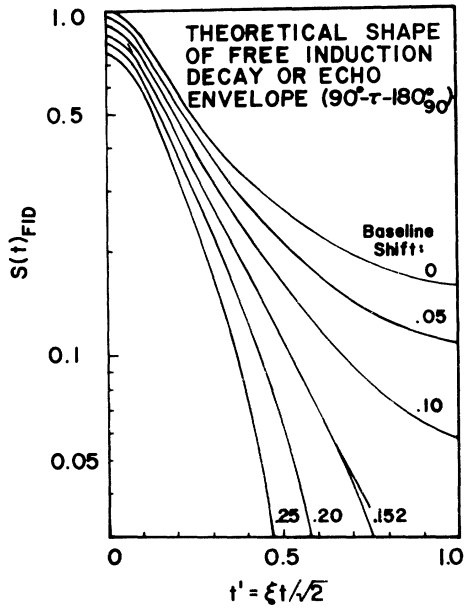

FIG. 2. Shape of the free induction decay or envelope of $90°$-τ-$180°_{90°}$ echoes for an $I=\frac{9}{2}$ rigid solid with a Gaussian electric-field-gradient distribution. The analysis shows that a normalized baseline shift of 0.152, the theoretical contribution from the central transition, yields a residual exponential decay shape over the region of the data.

Lorentzian and Gaussian field gradient distribution functions: $F_n^L = e^{-2n\lambda t}$ and $F_n^G = e^{-2n^2\xi^2 t^2}$. Here $S(2\tau)e^{-\delta(2\tau\pm t)}$ was assumed constant (unity) over the echo and the dimensionless time axes are $t'_L=\lambda t$ and $t'_G=\xi t/\sqrt{2}$. Although the data fit neither curve accurately, they more nearly satisfy that generated by a Gaussian $f(a)$. Thus, apparently even in the rigid lattice, the ^{83}Kr nuclei are simultaneously affected by a large number of defects.

The theoretical shape of the "rapid" part of the free induction decay, Eq. (3), for a Gaussian field gradient distribution $f(a)$ is given in Fig. 2. Also shown are several curves in which a constant has been subtracted from $S(t)_{FID}$. For spin $\frac{9}{2}$ the relative intensity of the $\frac{1}{2}\rightarrow-\frac{1}{2}$ central transition is $\frac{5}{33}=0.152$. Clearly, when the contribution from the central transition is removed (baseline shift $=0.152$), the decay is predicted to be exponential over a large interval. Thus provided the "slower" part of the free induction decay can be assumed constant over the region of the "rapid" decay, the two components are additively separable and can be described in terms of the two time constants T_{2q} and T_{2c}. That the dipolar broadening of the central transition may be described by a Lorentzian function even in the rigid lattice is discussed in Sec. III B. In Sec. III C physical meaning is

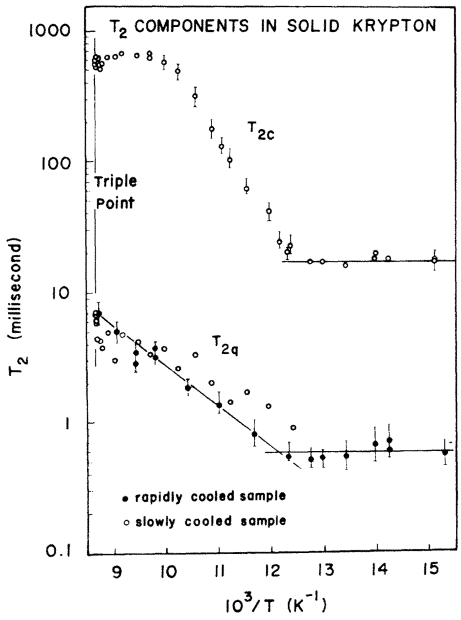

FIG. 3. Temperature dependence of the central (T_{2c}) and quadrupolar (T_{2q}) components of the spin-spin relaxation in solid krypton.

given to T_{2q} by empirically relating it to the half-width of the field gradient distribution.

B. Dipolar interaction

The spin-spin relaxation times T_{2c} and T_{2q} observed in solid krypton are plotted as functions of reciprocal temperature in Fig. 3. For both components regions of the rigid lattice and of motional narrowing may be identified. The onset of narrowing of the central component is found to occur at about 81 K ($10^3/T = 12.4$). Below this temperature, the data still exhibit a definite Lorentzian character with an exponential echo envelope decay constant of

$$T_{2c}^{rl}(\text{expt-Lorentzian}) = 17 \pm 3 \text{ msec}, \tag{6}$$

corresponding to a resonance half-width at half-maximum

$$\langle \Delta H_c \rangle_{rl} = 1/\gamma T_{2c}^{rl} = 0.056 \pm 0.010 \text{ G}. \tag{7}$$

We take

$$\omega_d \equiv 1/T_{2c}^{rl} = 59 \text{ sec}^{-1} \tag{8}$$

as a measure of the observed dipolar interaction strength.

The quadrupolar part T_{2q} of the spin-spin relaxation also is independent of temperature below about 80 K (Fig. 3). T_{2q} in this "rigid-lattice" region is 0.58 msec, which corresponds to a magnitude for the static quadrupolar interaction

$$\omega_q \equiv 1/T_{2q} = 1.7 \times 10^3 \text{ sec}^{-1}; \tag{9}$$

thus we have for ^{83}Kr in solid krypton

$$\omega_q/\omega_d \simeq 29. \tag{10}$$

The nuclear dipolar interaction on a fcc lattice is expected to produce a nearly Gaussian resonance line shape. Using the Van Vleck method of moments[20] and the usual truncated dipolar Hamiltonian, one obtains (for 11.55% ^{83}Kr at 40 K) a predicted second moment $M_2 = 7490$ sec^{-2} and corresponding Gaussian relaxation time $T_2^{rl} = 11.5$ msec. First-order quadrupolar coupling for $I = \frac{9}{2}$ modifies this moment by $\frac{1961}{1485}$ for the central transition and "like" spins and by $\frac{277}{297}$ for "semilike" spins[21] (experiencing different field gradients). A mean-value compromise yields the theoretical decay time constant

$$T_{2d}^{rl}(\text{theory-Gaussian}) = 11 \text{ msec}. \tag{11}$$

The effect of magnetic dilution on the rigid-lattice dipolar line shape can be considered by examining the fourth moment. Unfortunately, evaluation of M_4 is quite complicated for a fcc lattice, even in the nearest-neighbor approximation. Using Abragam's[22] formulation for a simple cubic lattice with the field along the [001] axis gives the moment ratio

$$M_4/3M_2^2 = 1.5, \tag{12}$$

which indicates only a slight deviation from a Gaussian line shape. By constructing a linear superposition of Gaussian and Lorentzian distributions satisfying Eqs. (6) and (12), one obtains a Lorentzian character of 7%. On the other hand, it turns out that such a superposition must be at least 50% Lorentzian in order for its transform to fit the observed echo envelopes within error bars. This would correspond to a moment ratio of $M_4/3M_2^2 \geq 100$.

The effect of the second-order quadrupole interaction on the central transition can be estimated using the interaction strengths discussed in Sec. III C. The central line will be shifted by this interaction when[1]

$$\omega_q^2/\omega_0 \simeq \omega_d. \tag{13}$$

In the present experiments, $\omega_q^2/\omega_0 \simeq 5 \times 10^{-2}$ sec^{-1}, which is much less than ω_d, and the effects of the second-order quadrupole interaction, as well as of magnetic dilution, are insufficient to account for the observed line shape, which remains only partially understood.

Figure 4 again presents the T_{2c} data of Fig. 3, together with a portion of the ^{83}Kr solid T_1 results published earlier.[5] The solid line has been normalized to the T_1 data at 80 K and drawn with the

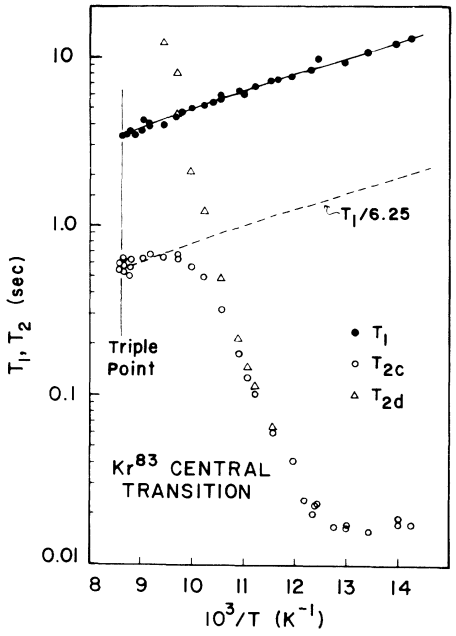

FIG. 4. T_2 for the central $\frac{1}{2} \rightarrow -\frac{1}{2}$ transition and correction for T_1-related cross relaxation.

temperature dependence predicted by Van Kranendonk and Walker[23] for quadrupolar relaxation by anharmonic Raman scattering of thermal phonons. A temperature-dependent Debye temperature has been employed.[5]

A striking feature of Fig. 4 is the apparent T_1 limitation of the ^{83}Kr T_{2c} relaxation times in the hot solid, but at a magnitude substantially smaller than T_1. In Sec. III A of the preceding paper Fedders[15] has shown that in the presence of a large first-order quadrupole interaction intraspin cross relaxation can arise from a quadrupolar T_1 process such as the thermal phonon-quadrupole mechanism[23] present in krypton. Fedders predicts that in the absence of other T_2 processes the central $\frac{1}{2} \rightarrow -\frac{1}{2}$ transition for spin $\frac{9}{2}$ should be characterized by the ratio $T_1/T_2 = 6.25$.

The lower dashed line in Fig. 4 corresponds to the solid line through the T_1 data, divided by 6.25. One sees a convincing agreement with the T_{2c} values observed in hot solid krypton near the melting point, where the motionally narrowed dipolar contribution to $1/T_2$ might be expected to have become negligible. Thus Fedders's prediction of significant T_2 effects arising from lowest-order quadrupole fluctuations is verified in krypton.

As a next step in the data analysis we examine the residual spin-spin relaxation time T_{2d} defined by

$$1/T_{2d} = 1/T_{2c} - 6.25/T_1 . \tag{14}$$

The T_{2d} values resulting from the T_{2c} data points and Eq. (14) are indicated as triangles in Fig. 4. We shall interpret T_{2d} as the spin-spin relaxation time arising from the motionally narrowed dipolar interaction for the ^{83}Kr central transition.

In Sec. III B of the preceding paper, Fedders[15] considers the case of motionally narrowed dipolar relaxation in the presence of first-order quadrupolar broadening with $\omega_0 \gg \omega_c \gg \omega_q \gg \omega_d$. He demonstrates that for spin $\frac{9}{2}$ the observed dipolar spin-spin relaxation rate will be larger than the usual theoretical rate by a multiplicative factor of 5.96.

For the case of a monovacancy diffusion process on a fcc lattice, Wolf[24] has shown that the spin-spin relaxation rate is given by

$$1/T_{2W} = 0.9628 f \alpha \tau / a_0^6 . \tag{15}$$

Here $f = 0.1155$ is the ^{83}Kr abundance, $\alpha = \frac{3}{2}\gamma^4\hbar^2 \times I(I+1)$, τ is the correlation time for atomic self-diffusion, and $2a_0 = r$ is the fcc cube-edge lattice parameter. $1/T_{2W}$ given by Eq. (15) is just $\frac{4}{3}$ times the Anderson-Weiss expression M_2/ω_c.

Fedders's modification of Eq. (15), to be applied to the ^{83}Kr T_{2d} data over the interval where $\omega_c \gg \omega_q$, yields

$$1/T_{2d} = 5.96/T_{2W} = 5.47 f \alpha \tau / a_0^6 . \tag{16}$$

It should be noted that in employing Fedders's theory the usual "like" or "semilike" coefficients should not be included in computing $1/T_{2d}$ for the motionally narrowed central component.

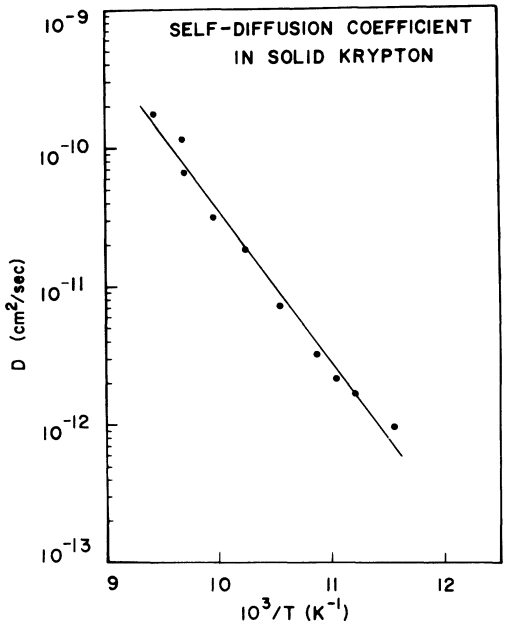

FIG. 5. Coefficient of atomic self-diffusion for solid krypton. The line indicated is a least-squares fit of an Arrhenius relation to the data.

We have used Eq. (16) and the T_{2d} data of Fig. 4 to calculate the corresponding values of τ. For diffusion on a fcc lattice one can write the coefficient of atomic self-diffusion $D = r^2/12\tau = a_0^2/3\tau$. In the calculation we have used the krypton lattice parameters of Losee and Simmons.[25] Figure 5 presents the coefficients D for solid krypton, corresponding to our T_{2d} results over the $10^3/T$ interval from 9.44 to 11.55. At higher temperatures T_{2d} becomes much larger than $6.25/T_1$ and at lower temperatures the condition $\omega_c \gg \omega_q$ is not satisfied. In the rigid lattice we observe a static quadrupolar interaction strength $\omega_q = 1.7 \times 10^3$ sec^{-1} [Eq. (9)]. Correspondingly, for the data point at $10^3/T = 11.55$ we find $\omega_c/\omega_q \simeq 2$, and inclusion of this point may extend the analysis beyond the region of validity of Fedders's calculations. At $10^3/T = 9.44$ we estimate $\omega_c/\omega_q \simeq 360$.

The line drawn in Fig. 5 is a least-squares fit of an Arrhenius relation, $D_0 \exp(-E_D/RT)$, to the data and corresponds to the result for atomic self-diffusion in solid krypton,

$$D = 3.1^{+6.8}_{-2.1} \exp[-(5010 \pm 220)/RT] \text{ cm}^2/\text{sec} . \quad (17)$$

The indicated error limits correspond to a rms standard deviation.

Our result can be compared with the self-diffusion parameters reported[11] from radioactive tracer measurements:

$$D = 5^{+5}_{-2} \exp[-(4800 \pm 200)/RT] \text{ cm}^2/\text{sec} . \quad (18)$$

The individual data points of Fig. 5 fall close to the tracer results reported[11] for a krypton sample containing 0.4% oxygen. However, we believe that our samples had less than 1.7-ppm O_2.

Application of the law of corresponding states[9,26] to NMR-determined xenon self-diffusion parameters[8] yields for krypton the predicted coefficient

$$D = 9.48^{+0.52}_{-0.25} \exp[-(5254 \pm 35)/RT] \text{ cm}^2/\text{sec} . \quad (19)$$

This result has been calculated from the xenon NMR-determined[8] diffusion coefficient corrected for lattice correlation and monovacancy encounter effects[24]:

$$D_{\text{xenon}} = 9.7^{+0.5}_{-0.3} \exp[-(7400 \pm 50)/RT] \text{ cm}^2/\text{sec} . \quad (20)$$

It has been pointed out[9,26] that a quantum-mechanical modification of the law of corresponding states successfully correlates the reduced activation energies for self-diffusion observed in the rare-gas solids. In both analyses it appears that the tracer-determined E_D for krypton, Eq. (18), falls some 10% below the correspondence curve.[11] The present NMR result, 5010 cal/mole, lies somewhat closer to the correspondence prediction, Eq. (19), but a more accurate NMR measurement would be desirable. Methods based on adiabatic demagnetization in the rotating reference frame (ADRF) recently have been employed in this laboratory to study very slow atomic motions in solid neon.[10] The ADRF apparatus now is being modified for use with a krypton sample isotopically enriched to 73% ^{83}Kr in an ADRF examination of slow motions in solid krypton. These new experiments should extend the present NMR determinations of the atomic diffusion coefficient in solid krypton to values several orders of magnitude smaller at temperatures near 70 K.

C. Quadrupole interaction

We have identified the rigid-lattice value of T_{2q} below 80 K with a magnitude ω_q for the static quadrupolar interaction, Eq. (9). It is not appropriate to relate ω_q to the second moment of the field gradient distribution, since, for a small concentration of defect gradient sources, the second moment will be dominated by spins adjacent to defects and will not be representative of the interaction for most nuclei. However, a resonance linewidth still can provide some measure of the quadrupolar interaction strength.

In the case where intraspin cross relaxation can be neglected, it has been shown[3] that a small concentration of randomly distributed defects leads to transient spin signals modified by multiplicative factors proportional to $e^{-|bt|^p}$, where b and p depend on the specific mechanism. Such an analysis is not appropriate for ^{83}Kr because of the mathematical complexity of the spin-$\frac{9}{2}$ case and because intraspin cross relaxation cannot be neglected.

A relationship between ω_q and the half-width of the effective electric-field-gradient distribution δa can be estimated from the quadrupole echo shape. Mehring and Kanert[19] have given a prescription for analyzing a compound echo when the form of $f(a)$ is known. When the mean quadrupole interaction is large compared to the mean dipole interaction, the reciprocal half-width of the quadrupole distribution function t_Q is related to the half-width t_s of the satellite contribution to the echo by $t_Q = \Gamma t_s$. For a Gaussian distribution and $I = \frac{9}{2}$, Γ is 3.84. From Eq. (4) and Fig. 1, one obtains $t_s = 0.211 \pm 0.010$ msec. Hence for a Gaussian $f(a)$ the corresponding half-width is

$$\delta a \equiv 1.177/t_Q = (1.45 \pm 0.07) \times 10^3 \text{ sec}^{-1} . \quad (21)$$

Thus an empirical relation between ω_q and δa in the krypton rigid lattice is given by

$$\delta a = 0.84 \omega_q . \quad (22)$$

Since the quadrupole broadening is not much larger than the magnet inhomogeneity, direct determination of δa from the quadrupole echo shape was not possible at temperatures above the onset of motional narrowing. However, for this region the temperature dependence of δa can be inferred from that of T_{2q}.

Motional narrowing of the quadrupolar structure is expected to occur much in the same way as the dipolar structure. At higher temperatures, diffusion processes create various environments for an atom. By analogy with the dipolar case, the onset of motional narrowing is expected to occur when the correlation time for the fluctuating gradients τ_g is of the order T_{2q}^{rl}.

The increase in T_{2q} with temperature in the narrowing region was found to be somewhat dependent on sample history. The data shown in Fig. 3 all were taken for decreasing temperature sequences in order to avoid effects of compression of the sample by the chamber. When the sample was cooled rapidly with large steps between successive temperatures, T_{2q} followed a thermally activated behavior, with

$$T_{2q} \propto \exp[-(1400 \pm 200 \text{ cal/mole})/RT]. \quad (23)$$

When the sample was cooled slowly, fluctuations in T_{2q} were observed. These fluctuations suggest the migration of defects into clusters which eventually collapse changing the defect concentration.

Losee and Simmons[25] have reported simultaneous length and x-ray lattice parameter measurements on well-annealed large-grained solid krypton samples. Their results show that $(\Delta l/l_0 - \Delta a/a_0)$ starts differing measurably from zero near 80 K. The data, interpreted as reflecting equilibrium atomic vacancy concentrations, indicate a concentration rising to about 0.3% at the triple point, with an enthalpy of formation of 1780 ± 200 cal/mole. At the pressures of the present experiments the enthalpy of vacancy formation is the same as E_f, the energy of formation, and one can write the fractional monovacancy concentration

$$n_v = \exp[2.0^{+1.0}_{-0.5} - (895 \pm 100)/T]. \quad (24)$$

Their experiments thus yield an activation energy for vacancy formation

$$E_f = 1780 \pm 200 \text{ cal/mole}, \quad (25)$$

and $n_v(82.5 \text{ K}) \simeq 1.4 \times 10^{-4}$, rising to $n_v \simeq 3 \times 10^{-3}$ near the triple point (115.8 K).

Since the present work shows no evidence of a motional T_{1q} in hot solid krypton, it is logical to associate the observed T_{2q} increase with adiabatic narrowing of a static quadrupolar broadening, or with a reduction in the static strength of the quadrupole interaction, as the defect sources of field gradients anneal out with increasing temperature.

The fact that the T_{2q} increase begins near 80 K might indicate a thermal vacancy origin for T_{2q}, especially since an adiabatic-narrowed vacancy interaction might be expected to exhibit an exponential $T_{2q}(T)$ variation with activation energy $(E_m - E_f)$. This could follow from a rate $1/T_{2q}$ proportional to n_v/ω_v, where one neglects atomic motion, since $\omega_v = \omega_a/n_v \gg \omega_a$ and n_v enters because the number of gradient sources increases as n_v. Such a model is particularly attractive since, using our $E_D = E_f + E_m = 5010$ cal/mole and $E_f = 1780$ cal/mole corresponds to $E_m - E_f = 1450$ cal/mole, in agreement with the observed T_{2q} temperature variation.

However, using either D from corresponding states, Eq. (19), or the present work, Eq. (17), one finds that $\omega_v = \omega_0 = 5.32 \times 10^7$ sec^{-1} at about 95 K ($10^3/T \simeq 10.5$), and so the adiabatic assumption is violated midway in the interval of the observed T_{2q} increase. Using the tracer result for D, $\omega_v = \omega_0$ near 86 K and the entire T_{2q} increase should then reflect extreme narrowing.

The T_{2q} fluctuations observed for slowly cooled samples support an alternative interpretation of a T_{2q} increase arising from a reduced static quadrupole interaction strength as temperature increases. Further work is required for a satisfactory understanding of the temperature variation of T_{2q}.

IV. RESULTS IN LIQUID

Extreme narrowing of both the dipolar and quadrupolar components of the spin spectrum was found to exist in the liquid phase. The resultant exponential spin-spin relaxation was found to be lifetime limited near the triple point, as shown in Fig. 6. The observed T_1 relaxation (reported previously[5]) and the experimental diffusion coefficient also are shown. A systematic deviation between T_1 and T_2 clearly exists near the critical point. This difference is well outside the combined uncertainties in the T_1 and T_2 measurements. Its source is not understood at this time.

The data do not follow an Arrhenius behavior over the entire liquid range. Below about 160 K, the diffusion coefficient is well described by

$$D = (103 \pm 17) \times 10^{-5} \exp[-(930 \pm 40)/RT] \text{ cm}^2/\text{sec}. \quad (26)$$

These data are about 50% larger than the radioactive-tracer diffusion data of Naghizadeh and Rice[12] over the same temperature range (dashed line in Fig. 6), but are described by about the same activation energy, $E_D(\text{tracer}) = 810$ cal/mole.

In the case of liquid xenon, NMR-determined

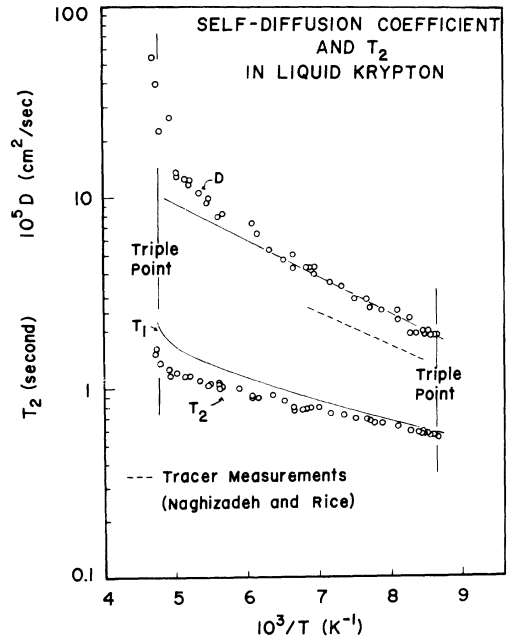

FIG. 6. Temperature dependence of the self-diffusion coefficient and T_2 of ^{83}Kr in liquid krypton. Previously reported T_1 results also are indicated.

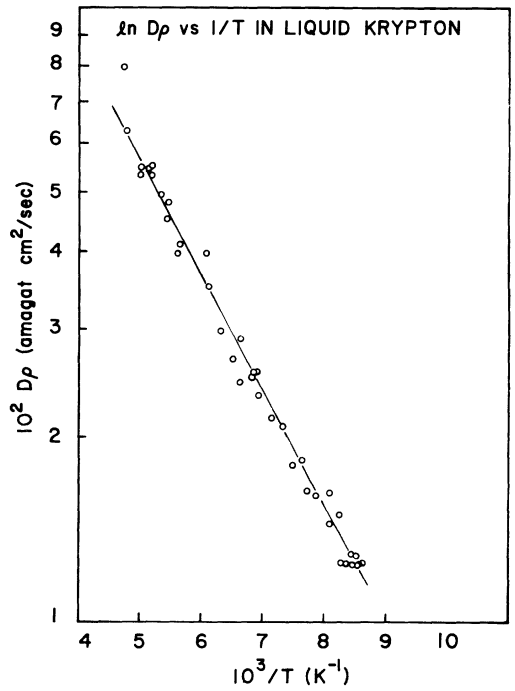

FIG. 7. Density-corrected self-diffusion coefficient in liquid krypton.

values[8] of D also were larger (by a factor of 2) than the tracer results of Naghizadeh and Rice.[12] However, in the case of liquid neon, NMR- determined values of D have been reported[9] in good agreement with tracer results reported by Bewilogua, Gladun, and Kubsch.[27] These results are summarized in Table I. Reduction of the krypton activation energy according to the law of corresponding states (using the Lennard-Jones potential parameters of Horton and Leech[28]) finds it in good agreement with the E_D^* obtained by NMR in the other rare-gas liquids.

In liquid krypton D is found to increase more rapidly than indicated by Eq. (26), for temperatures greater than 160 K. This deviation is in the opposite sense to the slight pressure dependence noted by Naghizadeh and Rice.[12] The increased diffusivity can, however, be accounted for as arising from the decrease in density with increasing temperature. A semilogarithmic plot of the product $D\rho$ vs reciprocal temperature is shown in Fig. 7. Except at the critical point, the data are well described by a thermally activated model with

$$D\rho = (48.7 \pm 6.8) \times 10^{-2} \times \exp[-(860 \pm 40)/RT] \text{ amagat cm}^2/\text{sec} = (1.83 \pm 0.25) \times 10^{-3} \times \exp[-(860 \pm 40)/RT] \text{ g/cm sec}. \quad (27)$$

The anomalous increase observed for D at the critical point may be genuine. However, in view of the large uncertainties in the densities near this point, such behavior cannot be confidently inferred from the present data.

TABLE I. Self-diffusion parameters for the rare-gas liquids (N = NMR, T = tracer).

	$10^5 D_0$ (cm^2/sec)	E_D (cal/mole)	E_D^*	Reference
Ne (N)	66^{+21}_{-16}	211 ± 15	2.99 ± 0.21	9
(T)	84.2 ± 2.8	225 ± 14	3.19 ± 0.20	27
Ar (T)	116	699	2.96	12
Kr (N)	103 ± 17	930 ± 40	2.85 ± 0.12	Present paper
(T)	48	803	2.43	12
Xe (N)	230^{+80}_{-70}	1400 ± 150	3.05 ± 0.32	8
(T)	70	1206	2.62	12

V. SUMMARY

The density matrix formalism was applied to a spin-$\frac{9}{2}$ solid and found to yield predictions in agreement with the observed double-exponential T_2 decay for ^{83}Kr in solid krypton. Conditions for this agreement are that the quadrupole interaction be strong relative to the dipole interaction and that the distribution of electric field gradients generated by lattice defects be Gaussian. The rms quadrupole splitting was determined from quad-

rupole echoes in the rigid solid and related to the time constant of the "rapid" part of the T_2 decay. The "slow" part was interpreted as reflecting the central $\frac{1}{2} \rightarrow -\frac{1}{2}$ transition.

The central line of the ^{83}Kr spectrum was found to exhibit several anomalies. A Lorentzian line shape was observed in the rigid solid, as opposed to an expected Gaussian. This is only partly accounted for by the dilute nature of the magnetic species and second-order quadrupole effects. Motional narrowing of this line commences near 80 K and continues until about 100 K, above which T_2 is limited by intraspin cross relaxation associated with the thermal phonon-quadrupolar T_1 process, as predicted by Fedders.[15] When the central component T_2 is corrected for this cross relaxation, the residual T_{2d} appears to reflect the motionally narrowed dipolar interaction and yields a reasonable value for the coefficient of atomic self-diffusion in solid krypton. The temperature variation of T_{2q} is not understood.

In the liquid, extreme narrowing of both components was observed, and at the triple point $T_2 \simeq T_1$. An unexplained deviation between T_1 and T_2 was found at higher temperatures.

The thermally activated model of self-diffusion was found to work well throughout the liquid range, provided compensation was made for the variation in density. Below 160 K the density changes slowly and the observed diffusion coefficient can be described by the Arrhenius relation.

ACKNOWLEDGMENT

The authors are indebted to Professor Peter A. Fedders for stimulating discussions and for comments on the manuscript.

---

*Based in part on the Ph.D. thesis presented by D. F. Cowgill to the Graduate School of Arts and Sciences, Washington University, 1971.

†Work supported by the Air Force Office of Scientific Research and the NSF.

‡Supported by a National Defense Education Act Fellowship and the National Aeronautics and Space Administration. Present address: Sandia Laboratories, Albuquerque, New Mexico.

[1]M. H. Cohen and F. Reif, in *Solid State Physics*, edited by F. Seitz and D. Turnbull (Academic, New York, 1957), Vol. 5.

[2]O. Kanert, D. Kotzur, and M. Mehring, Phys. Status Solidi 36, 291 (1969).

[3]Peter A. Fedders, Phys. Rev. B 11, 1020 (1975).

[4]M. K. Cueman, R. K. Hester, A. Sher, J. F. Soest, and I. J. Lowe, Phys. Rev. B 12, 3610 (1975).

[5]D. F. Cowgill and R. E. Norberg, Phys. Rev. B 8, 4966 (1973).

[6]W. W. Warren, Jr., and R. E. Norberg, Phys. Rev. 148, 402 (1966).

[7]W. W. Warren, Jr., and R. E. Norberg, Phys. Rev. 154, 277 (1967).

[8]W. M. Yen and R. E. Norberg, Phys. Rev. 131, 269 (1963).

[9]R. Henry and R. E. Norberg, Phys. Rev. B 6, 1645 (1972).

[10]B. E. Sirovich and R. E. Norberg, Bull. Am. Phys. Soc. 19, 273 (1974).

[11]A. V. Chadwick and J. A. Morrison, Phys. Rev. Lett. 21, 1803 (1968); Phys. Rev. B 1, 2748 (1970).

[12]J. Naghizadeh and S. A. Rice, J. Chem. Phys. 36, 2710 (1962).

[13]P. Carelli and I. Modena, Phys. Rev. A 7, 298 (1973).

[14]Portions of this work have been previously reported in preliminary form by D. F. Cowgill, Bull. Am. Phys. Soc. 16, 521 (1971).

[15]Peter A. Fedders, preceding paper, Phys. Rev. B 13, 2768 (1976).

[16]H. Y. Carr and E. M. Purcell, Phys. Rev. 94, 630 (1954).

[17]A similar expression can be written for a Gaussian dipolar broadening, etc; however, a Lorentzian shape appears more consistent with the experimental observations for ^{83}Kr (see Sec. III B).

[18]C. P. Slichter has shown that the spin-echo technique removes static magnetic gradients but not static electric ones [C. P. Slichter (private communication)].

[19]M. Mehring and O. Kanert, Z. Naturforsch. A24, 768 (1969).

[20]J. H. van Vleck, Phys. Rev. 74, 1168 (1948).

[21]K. Kambe and J. F. Ollom, J. Phys. Soc. Jpn. 11, 50 (1956).

[22]A. Abragam, *The Principles of Nuclear Magnetism* (Clarendon, Oxford, 1961), p. 125.

[23]J. van Kranendonk and M. B. Walker, Phys. Rev. Lett. 18, 70 (1967); Can. J. Phys. 46, 2441 (1968).

[24]D. Wolf, Phys. Rev. B 10, 2710 (1974).

[25]D. L. Losee and R. O. Simmons, Phys. Rev. 172, 934 (1968); 172, 944 (1968).

[26]W. E. Schoknecht, Ph.D. thesis (University of Illinois, 1971) (unpublished).

[27]L. Bewilogua, C. Gladun, and B. Kubsch, J. Low Temp. Phys. 4, 299 (1971).

[28]G. K. Horton and J. W. Leech, Proc. Phys. Soc. (Lond.) 82, 816 (1963).